

Electronic Transport in One-Dimensional Disordered Systems: Effects of the Finite-Size of the Impurities

Marlos Díaz *,¹ Pier A. Mello,¹ Miztli Yépez,² and Steven Tomsovic³

¹ *Instituto de Física, Universidad Nacional Autónoma de México,
Apartado Postal 20-364, México, D.F.*

² *Departamento de Física, Universidad Autónoma Metropolitana-Iztapalapa,
Apartado Postal 55-534, 09340, México, D.F.*

³ *Department of Physics and Astronomy,
Washington State University, Pullman, WA*

(Dated: December 7, 2024)

Abstract

We study the problem of electronic transport in a one-dimensional disordered system, where the impurities are modelled by scatterers consisting of n barriers and wells; these scatterers are assumed to have statistically independent intensities and a spatial extension l_c which may contain an arbitrary number $\delta/2\pi$ of wavelengths, where $\delta = kl_c$. We analyze the average Landauer resistance R/T and the average Landauer-Büttiker conductance T of the chain as a function of n and the phase parameter δ . For weak scatterers, we find: i) a regime, to be called I, associated with an exponential behavior of the resistance with n , ii) a regime, to be called II, for δ in the vicinity of π , where the system is almost transparent and less localized, and iii) right in the middle of regime II, for δ very close to π , an incipient “forbidden region”, which becomes ever more conspicuous as n increases. In regime II, both the average Landauer resistance and the transmission coefficient show an oscillatory behavior with n and δ . These characteristics of the system are found analytically and verified through numerical simulations, the agreement between the two being generally very good. This suggests a strong motivation for the experimental study of these systems.

PACS numbers: 72.10.-d, 73.23.-b, 73.63.Nm, 05.60.Gg

* Deceased

I. INTRODUCTION

The problem of electronic transport in disordered systems has been extensively studied in the literature, both for uncorrelated disorder (see, e.g., Ref.¹⁻⁸ and references therein), as well as for the case in which the disordered potential shows correlations^{2,9-15}.

Common features of the problems investigated by our group in Refs.^{7,8} are that i) uncorrelated disorder is contemplated, and ii) the size of the individual scatterers that compose the disordered system is the smallest one occurring in the problem: in particular, it is much smaller than the wavelength of the wave sent along the waveguide, and is thus of no physical relevance. In these models, each individual potential, statistically independent from the others, is modeled by a delta function, and the distance between successive scatterers is subsequently taken to be very small, which allows considering the so-called dense weak-scattering limit (DWSL), an important ingredient in the analysis carried out in those references. Various quantities of physical interest were investigated within this framework, like the conductance, its fluctuations, and the individual transmission coefficients of the disordered system. A particularly attractive property that was found is the insensitivity of the results to details of the individual-scatterer statistical distribution, expressed in the form of a central-limit theorem.

In the present paper we build on previous work¹⁶ to study the simplest extension of the problems contemplated in Refs.^{7,8}: the problem of electronic transport in 1D disordered systems, in which the impurities are modelled by scatterers having a finite size. Specifically, we consider a succession of barriers and wells, to be referred to, generically, as steps, having a finite width. The same model has been studied later in Ref.¹⁷, using a mapping to a “classical phase space” and iterating that map. The potential under study is shown schematically in Fig. 1 below. It contains n steps, assumed to be weak compared with the energy E . The steps are characterized by:

- i) A fixed width l_c which may fit an arbitrary number of wavelengths $\delta/2\pi$, where the parameter $\delta = kl_c$, k being the wave number, will be referred to as the *phase parameter*.
- ii) Random heights V_r ($r = 1, \dots, n$). The n heights V_r are statistically independent of one another; the n distributions are uniform, with zero average, and identical to one another.

We shall see that this simple model that contemplates a finite size of the scatterers exhibits peculiar transport properties¹⁶ which, to the best of our knowledge, have not been discussed

in the literature, and thus suggest their experimental verification in the laboratory. Although effects produced by the finite size of the scatterers or of their separation (as in “random Kronig-Penney models”) have been considered in the literature in various publications (see, e.g., Refs. [2,11,13,18] and references cited therein), they have not been discussed in the context considered here.

In this paper we study, for the model we just described, the dimensionless Landauer resistance R/T of the chain¹⁹ and its Landauer-Büttiker dimensionless conductance²⁰ $g = T$ (for “spinless” electrons; R and T are the reflection and transmission coefficients of the chain), averaged over an ensemble of realizations, as functions of the number of scatterers n and the phase parameter δ . (From now on, in this 1D problem we shall use interchangeably the terms “transmission coefficient” and “Landauer-Büttiker dimensionless conductance”.)

We perform a theoretical analysis of the problem outlined above and verify the results by means of computer simulations.

The paper is organized as follows. In the next section we describe the theoretical model using the transfer-matrix technique. Section III studies the exact theoretical results for the average Landauer resistance of the chain, as well as the results of computer simulations. We first discuss the average Landauer resistance as a function of the number of scatterers n for fixed values of δ , a novel feature of these results being their oscillatory behavior. We develop a perturbation theory for values of δ not too close to π , which gives a good understanding of the oscillations. We then discuss the average Landauer resistance as a function of δ for fixed n . The peculiarity here will be an “incipient forbidden region” found very close to $\delta = \pi$ (this region will be designated as $\delta \approx \pi$). In Sec. IV we perform a similar study for the average Landauer-Büttiker conductance of the chain. The theoretical results are subject to a number of approximations and are compared with computer simulations, the agreement between both being generally excellent. Just as in the case of the resistance, salient features of the results are, on the one hand, their oscillatory behavior and, on the other, the incipient forbidden region observed for $\delta \approx \pi$. We finally conclude in Sec. V. Three appendices are added in order not to interrupt the presentation in the main text.

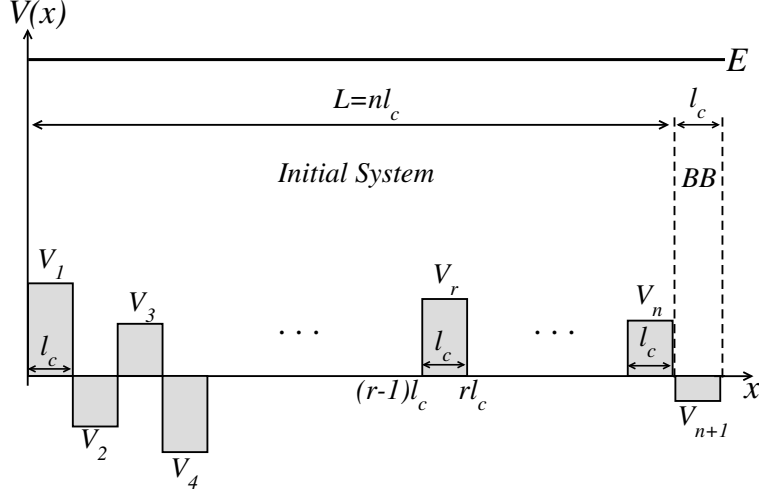


FIG. 1: Schematic representation of an array of n steps of random height V_r ($r = 1, \dots, n$) possessing a fixed spatial width l_c . The incident energy E is taken larger than all the $|V_r|$ ’s. Also indicated is the “initial system” with n scatterers and the addition of the BB consisting of the $n + 1$ -st scatterer.

II. THE THEORETICAL MODEL

In this section we give a theoretical treatment of the 1D system whose potential, represented schematically in Fig. 1, was described in the Introduction. The r -th scatterer of the chain is shown in Fig. 2 for the case of a barrier, $V_r > 0$; the definitions given below and in the figure also apply to a well, letting $V_r < 0$. In the region of the barrier, the energy \bar{E}_r and the wave number \bar{k}_r are given by

$$\bar{E}_r = E - V_r, \quad (2.1a)$$

$$(\bar{k}_r)^2 = k^2 - U_r, \quad (2.1b)$$

where

$$U_r = \frac{2mV_r}{\hbar^2}, \quad k^2 = \frac{2mE}{\hbar^2}. \quad (2.2)$$

We also introduce the dimensionless parameter

$$y_r = U_r l_c^2 = \frac{U_r}{k^2} (kl_c)^2 \equiv \frac{U_r}{k^2} \delta^2, \quad (2.3)$$

as a convenient measure of the intensity of the step potential.

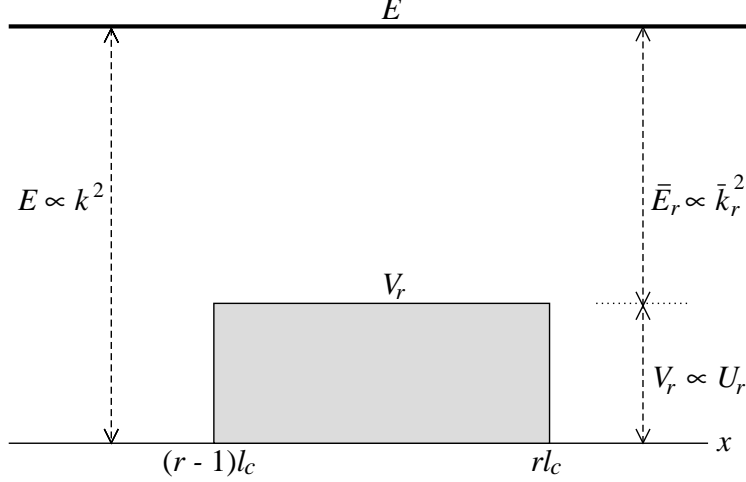


FIG. 2: Schematic representation of the r -th scatterer of the chain, for the case of a barrier. It has a fixed spatial width l_c and height V_r .

The transfer matrix for the r -th scatterer has the structure

$$\mathbf{M}_r = \begin{bmatrix} \alpha_r & \beta_r \\ \beta_r^* & \alpha_r^* \end{bmatrix}, \quad (2.4)$$

with the condition $|\alpha_r|^2 - |\beta_r|^2 = 1$, so that it fulfills the properties of flux conservation and time-reversal invariance⁷. For an incident energy E above a barrier ($0 < y_r < \delta^2$), or for arbitrary E in the case of a well, we find, from Schrödinger's equation

$$\alpha_r = e^{-i\delta} \left[\cos \left(\sqrt{\delta^2 - y_r} \right) + i \frac{2\delta^2 - y_r}{2\delta \sqrt{\delta^2 - y_r}} \sin \left(\sqrt{\delta^2 - y_r} \right) \right] \equiv \mathring{\alpha}_r, \quad (2.5a)$$

$$\beta_r = -ie^{-i(2r-1)\delta} \frac{y_r}{2\delta \sqrt{\delta^2 - y_r}} \sin \left(\sqrt{\delta^2 - y_r} \right) \equiv -ie^{-i(2r-1)\delta} \mathring{\beta}_r, \quad (2.5b)$$

where the quantities $\mathring{\alpha}_r$ and $\mathring{\beta}_r$ are independent of the “running-phase” factor $\exp(-2ir\delta)$. The transfer matrix associated with a chain containing n (non-overlapping) steps will be denoted by

$$\mathbf{M}^{(n)} = \mathbf{M}_n \cdots \mathbf{M}_r \cdots \mathbf{M}_2 \mathbf{M}_1 = \begin{bmatrix} \alpha^{(n)} & \beta^{(n)} \\ (\beta^{(n)})^* & (\alpha^{(n)})^* \end{bmatrix}, \quad (2.6)$$

where lower indices refer to individual scatterers. Quantities of particular physical interest are the dimensionless Landauer resistance¹⁹ $\lambda^{(n)}$ of the chain

$$\lambda^{(n)} = |\beta^{(n)}|^2 = \frac{R^{(n)}}{T^{(n)}} \quad (2.7a)$$

and its dimensionless Landauer-Büttiker conductance²⁰ given by the transmission coefficient

$$g^{(n)} = T^{(n)} = \frac{1}{1 + \lambda^{(n)}}. \quad (2.7b)$$

Here, $\lambda^{(n)}$ is the “radial” parameter in the polar representation of the transfer matrices⁷.

The ensemble of chains described in the Introduction is defined by assuming that the y_r ’s ($r = 1, \dots, n$) are statistically independent of one another, each being uniformly distributed in the interval $(-y_0, y_0)$. This is equivalent to saying that, for fixed l_c , each U_r is uniformly distributed in the interval $(-U_0, U_0)$, with $y_0 \equiv U_0 l_c^2$. If each chain is represented as in Eq. (2.6), the ensemble of chains is described by an *ensemble of transfer matrices*.

It is relevant here to comment on the dependence of the physical quantities of interest on the parameters that we have introduced. Notice that, although the transfer matrix for a single scatterer depends, in principle, on the three parameters E, U_r, l_c , Eqs. (2.5) show that these parameters occur in the combinations δ and y_r . Thus, for the full chain of n scatterers and a specific realization of disorder, a quantity like the transmission coefficient $T^{(n)}$ depends on the various parameters as

$$T^{(n)} = f(\delta, n, y_1, \dots, y_n). \quad (2.8)$$

Its ensemble average is thus given by

$$\langle T^{(n)} \rangle = \int \dots \int f(\delta, n, y_1, \dots, y_n) p_{y_0}(y_1) \dots p_{y_0}(y_n) dy_1 \dots dy_n \quad (2.9a)$$

$$= F(\delta, n, y_0), \quad (2.9b)$$

which is seen to depend on the three parameters δ, n and y_0 only.

III. AVERAGE LANDAUER RESISTANCE

We assume that the original system of n scatterers is extended with the addition of one scatterer, to be called a “*building block*” (BB), as shown in Fig. 1. The resulting transfer matrix is given by

$$\mathbf{M}^{(n+1)} = \mathbf{M}_{n+1} \mathbf{M}^{(n)}. \quad (3.1)$$

From this combination rule we find a recursion relation for Landauer's resistance of the chain, averaged over the ensemble, as

$$\begin{aligned} \left[1 + 2\langle|\beta^{(n+1)}|^2\rangle\right] - \left[1 + 2\langle|\beta^{(n)}|^2\rangle\right] &= 2\langle|\beta_{n+1}|^2\rangle \left[1 + 2\langle|\beta^{(n)}|^2\rangle\right] \\ &\quad + 2\left[\langle\alpha_{n+1}\beta_{n+1}^*\rangle\langle\alpha^{(n)}\beta^{(n)}\rangle + \text{c.c.}\right], \end{aligned} \quad (3.2a)$$

$$\begin{aligned} \langle\alpha^{(n+1)}\beta^{(n+1)}\rangle - \langle\alpha^{(n)}\beta^{(n)}\rangle &= \langle\alpha_{n+1}\beta_{n+1}\rangle \left[1 + 2\langle|\beta^{(n)}|^2\rangle\right] \\ &\quad + (\langle\alpha_{n+1}^2\rangle - 1) \langle\alpha^{(n)}\beta^{(n)}\rangle + \langle\beta_{n+1}^2\rangle\langle\alpha^{(n)}\beta^{(n)}\rangle^*, \end{aligned} \quad (3.2b)$$

where c.c. stands for “complex conjugate”. Notice that the above equations couple the average resistance of the chain, $\langle|\beta^{(n)}|^2\rangle$, to the quantity $\langle\alpha^{(n)}\beta^{(n)}\rangle$. The recursion relations (3.2) are exact, and thus take into account all multiple scattering processes occurring in the chain.

With the definitions

$$A(n) = 1 + 2\langle|\beta^{(n)}|^2\rangle, \quad (3.3a)$$

$$b(n) = e^{2in\delta}\langle\alpha^{(n)}\beta^{(n)}\rangle, \quad (3.3b)$$

we write Eqs. (3.2) as

$$\begin{bmatrix} \frac{A(n+1)}{2} \\ \frac{ib(n+1)}{\sqrt{2}} \\ -\frac{ib^*(n+1)}{\sqrt{2}} \end{bmatrix} = \begin{bmatrix} 1 + 2\langle|\dot{\beta}_1|^2\rangle & \sqrt{2}e^{i\delta}\langle\dot{\alpha}_1\dot{\beta}_1\rangle & \sqrt{2}e^{-i\delta}\langle\dot{\alpha}_1\dot{\beta}_1\rangle^* \\ \sqrt{2}e^{i\delta}\langle\dot{\alpha}_1\dot{\beta}_1\rangle & e^{2i\delta}\langle\dot{\alpha}_1^2\rangle & \langle\dot{\beta}_1^2\rangle \\ \sqrt{2}e^{-i\delta}\langle\dot{\alpha}_1\dot{\beta}_1\rangle^* & \langle\dot{\beta}_1^2\rangle & e^{-2i\delta}\langle\dot{\alpha}_1^2\rangle^* \end{bmatrix} \begin{bmatrix} \frac{A(n)}{2} \\ \frac{ib(n)}{\sqrt{2}} \\ -\frac{ib^*(n)}{\sqrt{2}} \end{bmatrix}, \quad (3.4a)$$

or, in an abbreviated form,

$$z(n+1) = \Omega_{y_0}(\delta)z(n). \quad (3.4b)$$

We have assumed that all the individual scatterers are equally distributed, so that the various BB averages are evaluated for the first scatterer. In Eq. (3.4b), $z(n)$ and $\Omega_{y_0}(\delta)$ are, respectively, the three-dimensional vector and the 3×3 matrix appearing on the right-hand side of Eq. (3.4a). The matrix $\Omega_{y_0}(\delta)$, which depends on y_0 and δ , will be denoted by Ω , for short, when no confusion arises. The various BB averages appearing in Ω are to be evaluated using the expressions of Eqs. (2.5).

The matrix Ω we have defined is *complex symmetric* and *independent of n* . Thanks to this last property, the solution of Eq. (3.4b) for arbitrary n can be written as

$$z(n) = \Omega^n z(0) \quad (3.5a)$$

$$z(0) = [1/2, 0, 0]^T, \quad (3.5b)$$

T meaning transposed. In particular (for some of the details, see App. A), using the initial condition (3.5b) and Eq. (A5) we find, for $A(n)$

$$A(n) = \sum_{a=1}^3 (O_{1a})^2 (\mu_a)^n, \quad (3.6a)$$

O being the complex orthogonal matrix that diagonalizes Ω (assuming that Ω has no double characteristic values). We notice that only the first component of each of the three eigenvectors enters the expression for $A(n)$. For the average Landauer resistance [see Eqs. (2.7a) and (3.3a)] we obtain

$$\langle \lambda^{(n)} \rangle = \frac{1}{2} [A(n) - 1]. \quad (3.6b)$$

It is often useful to write the matrix $\Omega_{y_0}(\delta)$ as

$$\Omega_{y_0}(\delta) = \Omega_0(\delta) + \Delta\Omega_{y_0}(\delta), \quad (3.7a)$$

$$\Omega_0(\delta) = \begin{bmatrix} \mu_1^{(0)} & 0 & 0 \\ 0 & \mu_2^{(0)} & 0 \\ 0 & 0 & \mu_3^{(0)} \end{bmatrix} = \begin{bmatrix} 1 & 0 & 0 \\ 0 & e^{2i\delta} & 0 \\ 0 & 0 & e^{-2i\delta} \end{bmatrix}, \quad (3.7b)$$

the unperturbed matrix $\Omega_0(\delta)$ being the limiting value of $\Omega_{y_0}(\delta)$ in the absence of a potential, i.e., for $y_0 = 0$.

A. Average Landauer resistance in regime I, as function of the number of scatterers n

Assume δ is far from π . E.g., for $\delta = \pi/2$, the three unperturbed eigenvalues of Ω_0 are $\{\mu_1^{(0)}, \mu_2^{(0)}, \mu_3^{(0)}\} = \{1, -1, -1\}$. We call *regime I* the region in which $\{\mu_2^{(0)}, \mu_3^{(0)}\}$ are far away from $\mu_1^{(0)}$, so that they may be considered effectively decoupled when we turn on a

weak interaction, $y_0^2 \ll 1$. We then restrict ourselves to the 1×1 block of Ω in Eq. (3.4a) consisting of the 11 matrix element, and write the solution, Eq. (3.5a), as

$$A(n) \approx \Omega_{11}^n A(0) = (1 + 2\langle |\beta_1|^2 \rangle)^n = e^{2n \frac{1}{2} \ln(1 + 2\langle |\beta_1|^2 \rangle)} \equiv e^{2nl_c/\ell}, \quad (3.8)$$

which defines the parameter ℓ , to be interpreted below. Eq. (3.8) is the well known exponential behavior found by Landauer¹⁹, where, in the present case,

$$\frac{l_c}{\ell} = \frac{1}{2} \ln(1 + 2\langle |\beta_1|^2 \rangle), \quad (3.9)$$

where β_1 refers to the first scatterer. In the WSL, $\langle |\beta_1|^2 \rangle = \langle R_1/T_1 \rangle \ll 1$, and we can write

$$\frac{l_c}{\ell} \approx \langle |\beta_1|^2 \rangle = \langle R_1/T_1 \rangle \approx \langle R_1 \rangle, \quad (3.10a)$$

so that

$$\frac{1}{\ell} \approx \frac{\langle R_1 \rangle}{l_c}. \quad (3.10b)$$

Thus $1/\ell$ is, approximately, the reflection coefficient per unit length, that we shall identify with the inverse of the *mean free path* (mfp)⁸, which, in the present 1D problem, is of the order of the localization length.

Explicitly, Landauer's resistance for the chain consisting of n scatterers in regime I takes the form

$$\langle |\beta^{(n)}|^2 \rangle = \frac{1}{2} (e^{2nl_c/\ell} - 1). \quad (3.11)$$

Using Eq. (2.5b), we can express $\langle |\beta_1|^2 \rangle$ appearing in (3.9) as function of δ and y_0 as

$$\langle |\beta_1|^2 \rangle = \left\langle \frac{y_1^2}{4\delta^2(\delta^2 - y_1)} \sin^2 \left(\sqrt{\delta^2 - y_1} \right) \right\rangle. \quad (3.12)$$

Although this average can be computed analytically and expressed in terms of cosine-integral functions, in future calculations it will be more convenient to compute it numerically. However, it is worth noticing that in the WSL it can be expanded in powers of y_0/δ^2 , giving the rather compact and transparent expression

$$\langle |\beta_1|^2 \rangle = \frac{l_c}{\ell} + O\left(\frac{y_0}{\delta^2}\right)^4, \quad \frac{l_c}{\ell} = \frac{y_0^2}{12\delta^4} \sin^2 \delta. \quad (3.13)$$

Notice that in the present problem *the mfp depends on the phase parameter δ* .

We now compare the theoretical result (3.11) with numerical simulations. In the WSL we have $y_0/\delta^2 \ll 1$; we fix $y_0 = 0.09$ and consider δ in the interval $(1, 2.9)$. Figure 3 shows

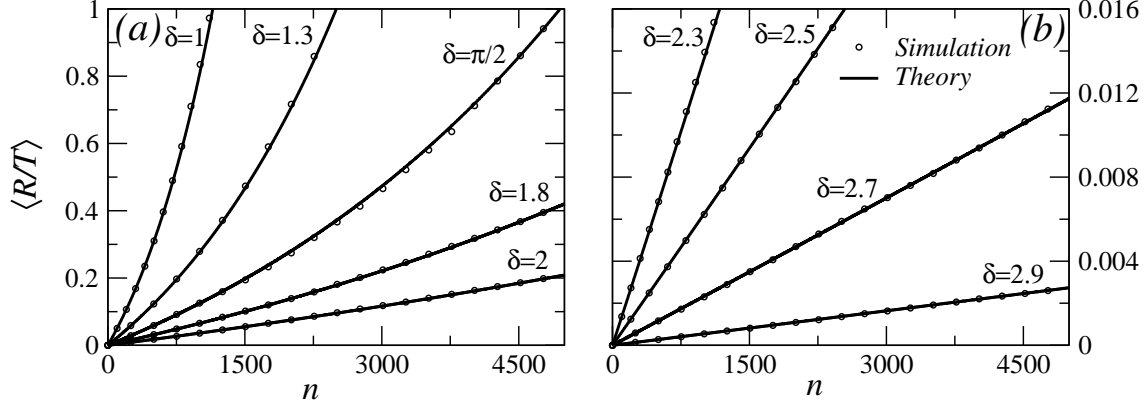


FIG. 3: Comparison between theory and computer simulations for the average Landauer resistance $\langle(R/T)^{(n)}\rangle$ as a function of the number n of scatterers for the 1D system described in the text. For the numerical simulation, an ensemble of 10^4 realizations was used. Results are shown in regime I for a number of δ 's: (a) $1 < \delta < 2$, (b) $2.3 < \delta < 2.9$. Notice the different scale in the ordinate of the two panels. We chose the parameter $y_0 = 0.09$ [the parameter related to the average step strength: see below Eqs. (2.7)]. The theoretical results are those given in Eq. (3.11), using the approximation (3.13) for the mfp. In the figure we cannot notice the difference between the two results. The error bar due to the finite sample size is very small and is not indicated in the figure: e.g., for $\delta = \pi/2$ and $n = 5000$, the error is $\sim 10^{-2}$. As δ increases, the average resistance decreases and the mfp increases: i.e., the system delocalizes.

the theoretical results and numerical simulations for the average Landauer resistance as functions of the length n of the chain, for various values of δ in the above interval: the agreement is excellent, indicating that the decoupling leading to the simple equation (3.11) for the resistance, as well as the expression (3.13) for the mfp are very good approximations.

The results indicate the *tendency of the system to delocalize, with a corresponding increase in the mfp, as the phase parameter δ increases towards π .*

B. Average Landauer resistance in regime II, as function of the number of scatterers n

In the region $2.9 \lesssim \delta \lesssim 3.4$, $\{\mu_2^{(0)}, \mu_3^{(0)}\}$ are not far enough away from $\mu_1^{(0)}$ to be effectively decoupled. We shall see that *a novel behavior shows up as a consequence of the coupling.*

1. The behavior of the average resistance for $\delta = \pi$

For $\delta = \pi$, the three $\mu_a^{(0)}$ are degenerate and equal to 1. In this case, and for weak scattering, i.e., $y_0 \ll 1$, Ω takes the approximate form

$$\Omega_{y_0}(\pi) \approx I + y_0^2 \Omega_{red} \quad (3.14a)$$

$$\Omega_{red} = \frac{1}{12\pi^3} \begin{bmatrix} 0 & -\sqrt{2} & -\sqrt{2} \\ -\sqrt{2} & -(2\pi + i) & 0 \\ -\sqrt{2} & 0 & -(2\pi - i) \end{bmatrix}, \quad (3.14b)$$

where Ω_{red} is approximately (i.e., for $y_0 \ll 1$) independent of y_0 . In the present case, $\Delta\Omega_{y_0}(\delta)$ of Eq. (3.7a) is $\Delta\Omega_{y_0}(\delta) = y_0^2 \Omega_{red}$.

Theoretical results (obtained diagonalizing Ω of (3.14) numerically) and computer simulations for the average Landauer resistance for $\delta = \pi$ are shown in Fig. 4 as a function of n . The excellent agreement between the two results indicates that writing Ω as in Eqs. (3.14) is a good approximation. Results for values of δ in regime I, taken from Fig. 3(b), are shown for comparison. What we learn is that the system is *less delocalized for $\delta = \pi$ than for neighboring values of δ* : i.e., *the tendency to delocalize as δ move towards π is reversed for $\delta = \pi$* . Take $n = 5000$ scatterers: as a result of the coupling, the resistance shows an *enhancement* at $\delta = \pi$, compared with neighboring values of δ , as shown in Fig. 4.

2. Perturbation theory for δ not too close to π

For δ not too close to π , so that the unperturbed eigenvalues do not become degenerate, we may use perturbation theory (PT) in the parameter y_0 to find approximate expressions for the eigenvalues and eigenvectors of the matrix Ω appearing in the recursion relation (3.4). We write $\Omega_{y_0}(\delta)$ as in Eqs. (3.7) and consider $\Delta\Omega_{y_0}(\delta)$ as a perturbation; the latter contains the BB expectation values appearing in Eq. (3.4a). The perturbation can be calculated analytically in leading order in y_0^2 , as we did with $\langle |\beta_1|^2 \rangle$, Eq. (3.13). However, just as we mentioned right below Eq. (3.12), it is convenient to have an exact expression for these BB quantities, so as to have a better control on the perturbation expansion: they were thus evaluated numerically.

We consider the eigenvalue equation

$$\Omega \mathbf{v}_i = \mu_i \mathbf{v}_i, \quad i = 1, 2, 3. \quad (3.15)$$

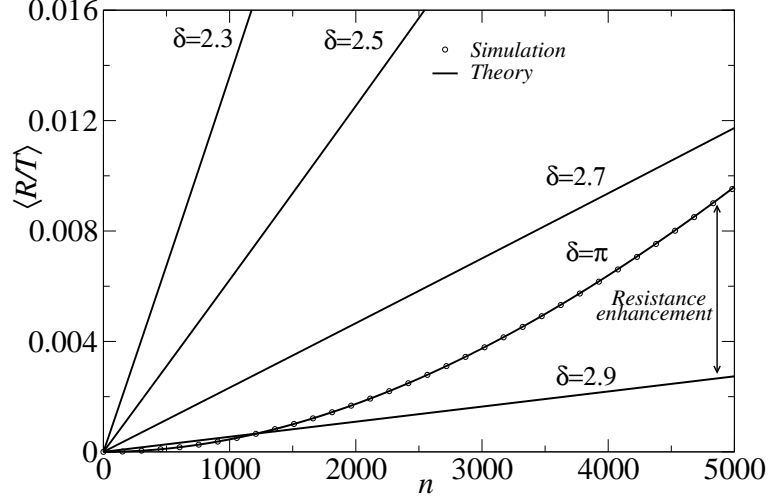


FIG. 4: For the same system as in Fig. 3, theoretical results from Eqs. (3.14) and computer simulations are shown, for $\delta = \pi$. The agreement is excellent. Results in the interval $2.3 < \delta < 2.9$ (regime I), taken from Fig. 3(b), are shown for comparison. The system is less delocalized for $\delta = \pi$ than for neighboring values of δ . As a result, the resistance is enhanced as $\delta = \pi$ is approached. The error bar is again so small that is not included in the figure.

The eigenvectors \mathbf{v}_i were previously designated as the columns of the matrix O of Eq. (A2), as in Eq. (3.6a). The perturbation theory used to solve approximately the above eigenvalue equation is briefly developed in App. B.

The quantity $A(n)$ of Eq. (3.6a) can be written in terms of the above eigenvectors as

$$A(n) = \mu_1^n (\mathbf{v}_1)_1^2 + \mu_2^n (\mathbf{v}_2)_1^2 + \mu_3^n (\mathbf{v}_3)_1^2, \quad (3.16)$$

where $(\mathbf{v}_i)_1$ designates component 1 of the eigenvector \mathbf{v}_i . Substituting the results of App. B, we can verify the identity $A(0) = 1$ up to second order in $\Delta\Omega$.

Fig. 5 shows the results of perturbation theory and simulations for the average Landauer resistance as a function of n , for four values of δ . A salient novel feature of these results is their *oscillatory behavior as a function of n* ; in the case of scatterers with a vanishing size and for a fixed wavelength as in previous studies⁸, oscillations with the present origin were absent. This behavior can be understood as follows. From Eq. (3.16), $A(n)$ has the structure

$$A(n) \sim A_1 e^{n \ln(1 + \Delta\mu_1)} + \left[A_2 e^{n \ln(e^{2i\delta} + \Delta\mu_2)} + cc \right], \quad (3.17)$$

where A_1, A_2 are constants independent of n and $\Delta\mu_i = \mu_i - \mu_i^{(0)}$. For $\delta = \pi + \epsilon$ and

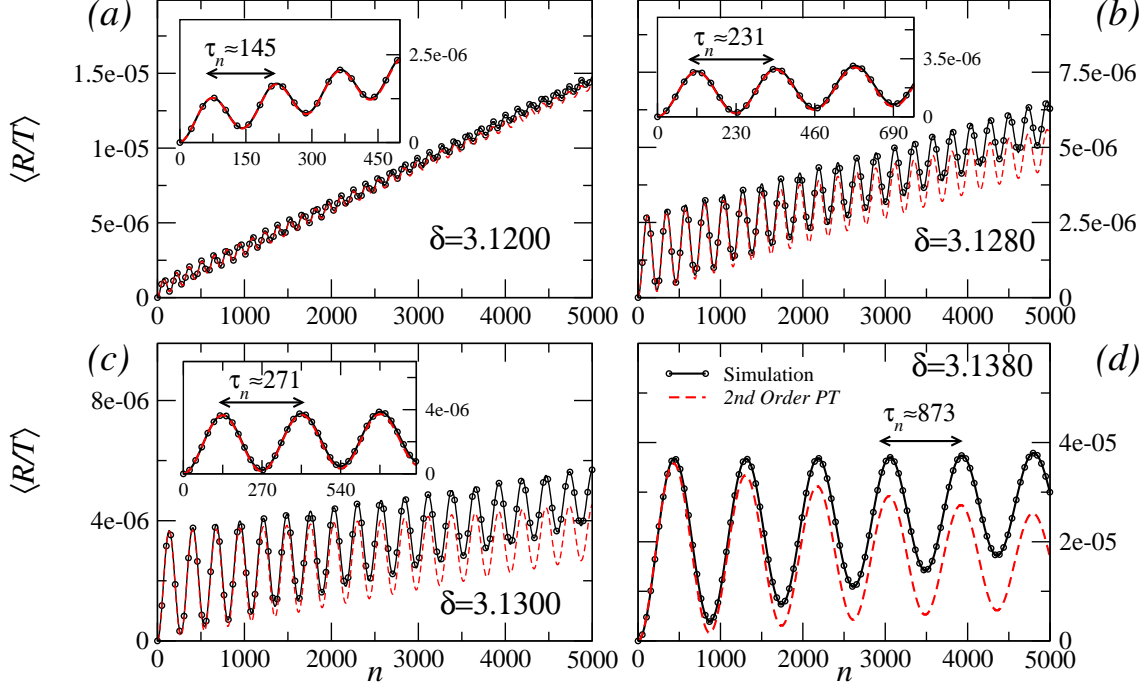


FIG. 5: Results of perturbation theory and computer simulations for the average Landauer resistance as a function of the number n of scatterers, for $\delta = 3.1200, 3.1280, 3.1300, 3.1380$ and, as usual, $y_0 = 0.09$. The matrix elements of $\Delta\Omega$ of the perturbation used in the calculation are essentially exact, as they were calculated numerically. Perturbation theory was carried out up to second order in $\Delta\Omega$ in the eigenvalues and the eigenvectors. The description is reasonable, especially in the first three cases (a,b and c); in the fourth case (d) the agreement deteriorates, as δ is too close to π . Notice the oscillatory behavior as a function of n . The insets in (a), (b) and (c) are a zoom of the results for the first few oscillations. The estimate of the period from Eq. (3.19) is indicated in each panel and is consistent with the numerical data.

neglecting $\Delta\mu_i$,

$$e^{n \ln e^{2i\delta}} = e^{n2i\delta} = e^{2in(\pi+\epsilon)} = e^{2in\epsilon}. \quad (3.18)$$

This result oscillates with n , with a period τ_n that satisfies $2\epsilon\tau_n = 2\pi$, so that, for δ fixed, we estimate

$$\tau_n \sim \frac{\pi}{\epsilon}. \quad (3.19)$$

This estimate for the period τ_n is independent of y_0 , it decreases as δ moves away from $\delta = \pi$, and is consistent with the results of Fig. 5.

3. Exact solution for δ very close to π ($\delta \approx \pi$)

If δ is very close to π , perturbation theory fails and Ω has to be diagonalized exactly. This has been done for a number of cases, shown in Fig. 6. The analytical results are a

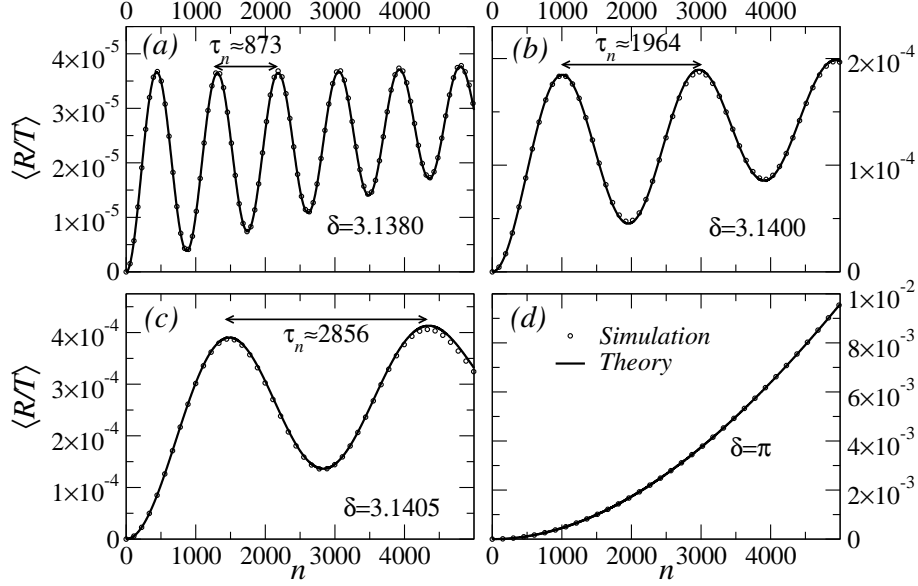


FIG. 6: Numerical simulations and analytical solution, Eqs. (3.6), for the average Landauer resistance $\langle R/T \rangle$ vs. n , obtained diagonalizing numerically the matrix $\Omega_{y_0}(\delta)$, for $y_0 = 0.09$ and for four values of $\delta \approx \pi$: (a)-(c) $\delta = 3.1380, 3.1400, 3.1405$; (d) $\delta = \pi$. The analytical solution is essentially exact. The results are symmetric around $\delta = \pi$ in the vicinity of this value. As a verification of the theoretical results, also shown are computer simulations using an ensemble of 10^4 realizations. For $\delta = \pi$, the statistical error bar is smaller than 10^{-5} and is not indicated. The estimate from Eq. (3.19) of the period τ_n of the oscillations is indicated in each panel and is consistent with the numerical simulations and the analytical results.

plot of the solution for the average Landauer resistance given in Eqs. (3.6), in which the matrix $\Omega_{y_0}(\delta)$ was diagonalized numerically. These results, which are essentially exact, have been verified with the aid of computer simulations, also shown in the figure. Notice again the oscillatory behavior of the resistance as a function of n : the period τ_n of the oscillations decreases as δ goes away from π , as we already noted in relation with Eq. (3.19).

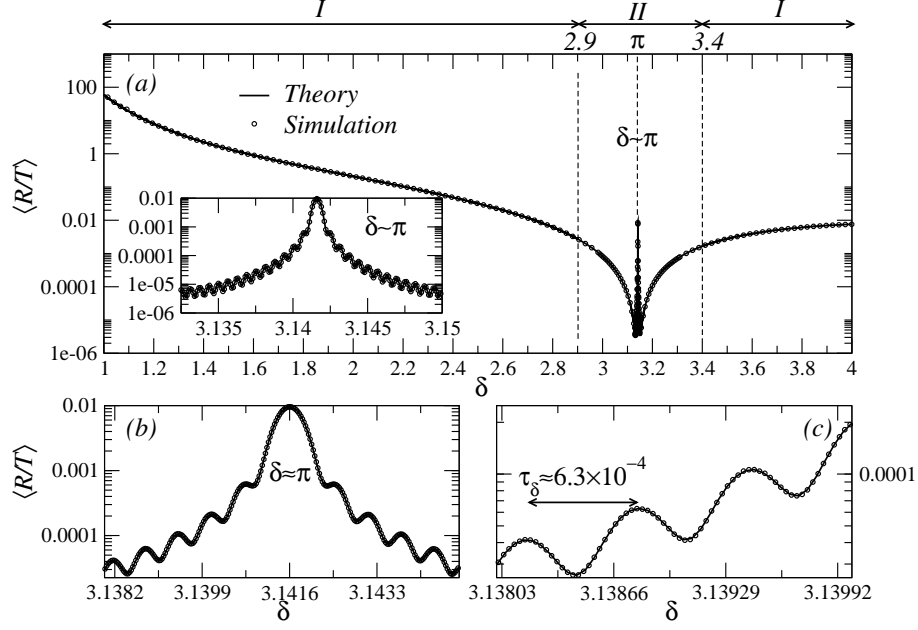


FIG. 7: Theory and numerical simulations for the average Landauer resistance $\langle R/T \rangle$ as a function of δ , for a chain of $n = 5000$ scatterers and for $y_0 = 0.09$, in regimes I and II. The simulations use 10^5 realizations. In regime I, the theoretical results given in Eqs. (3.11) and (3.13) were used: they agree very well with the simulations. In regime II, Eqs. (3.6) were employed, diagonalizing numerically the matrix Ω ; the computer simulations (with a statistical error bar $\sim 10^{-5}$ for $\delta = \pi$) constitute a verification of the theoretical results. Well inside regime II, we observe an enhancement of the average resistance by nearly *three orders of magnitude*, showing the existence of an incipient “forbidden region”. The inset in panel a), and panels b) and c) show this latter region in greater detail. Notice the *oscillatory behavior of the average Landauer resistance as a function of δ for fixed n* . The period of the oscillations can be estimated from Eq. (3.20) as $\tau_\delta \sim 6 \cdot 10^{-4}$, which is consistent with what we observe in the figure (in spite of δ being quite close to π).

C. Average Landauer resistance in regimes I and II, as function of δ for fixed n

We gain a global picture of the two regimes if we study the behavior of the average resistance $\langle R/T \rangle$ for a fixed length n of the chain, as a function of the phase parameter δ .

Fig. 7 shows the analytical results for $n = 5000$ scatterers and $1 < \delta < 4$, covering regimes I and II. We observe in Fig. 7a that the average resistance decreases as δ moves towards π , in agreement with the picture we have described of the system becoming more delocalized. The theoretical curve corresponding to regime I ($1 < \delta < 2.9$ and $\delta > 3.4$) was

again obtained from Eq. (3.11), and compares very well with the simulation.

In Regime II, the matrix Ω was diagonalized as before, and the result was introduced into Eqs. (3.6); these results were verified by computer simulations, also shown in Fig. 7. Well inside regime II the tendency of the average resistance to decrease as δ moves towards π is reversed: the figure shows the existence of an “*incipient forbidden region*”, in the sense that: i) in the very vicinity of $\delta = \pi$ the resistance presented by the system suffers a dramatic enhancement of nearly three orders of magnitude²¹ (see inset in panel (a)), ii) the peak-to-valley enhancement in the resistance keeps becoming greater for larger n ’s, as shown in an example in Fig. 8. This effect results from the coherent contribution of all the barriers and wells: we believe it to be a consequence of the barriers and wells having the same width l_c . Notice that the peak at $\delta = \pi$ shown in Fig. 7 is the same as the one shown in Fig. 4 for $n = 5000$. Fig. 4 shows that the average Landauer resistance for $\delta = 2.9$ increases with n according to Landauer’s formula (3.11), whereas for $\delta = \pi$ the increase with n is faster.

The inset in panel (a) of Fig. 7 exhibits an *oscillatory behavior of the average Landauer resistance as a function of δ for fixed n* . Again, this effect was not there in earlier studies in which the scatterers had a vanishing size. We can estimate the period from Eq. (3.18) as

$$\tau_\delta \sim \frac{\pi}{n}, \quad (3.20)$$

if δ is not too close to π .

IV. AVERAGE LANDAUER-BÜTTIKER CONDUCTANCE

A. Average Landauer-Büttiker conductance in regime I as function of the number of scatterers n

In this section we analyze the average Landauer-Büttiker dimensionless conductance $\langle g \rangle = \langle T \rangle$ (for “spinless” electrons) in regime I for the chains that we have been studying. Since for this quantity we have not succeeded in finding a recursion relation of the type obtained in Eqs. (3.4) for the average Landauer resistance, we resort to an approximate treatment.

From Eq. (3.8), valid in regime I, and treating n approximately as a continuous variable, we write

$$\frac{\partial A(n)}{\partial n} \approx 2 \frac{l_c}{\ell} A(n). \quad (4.1)$$

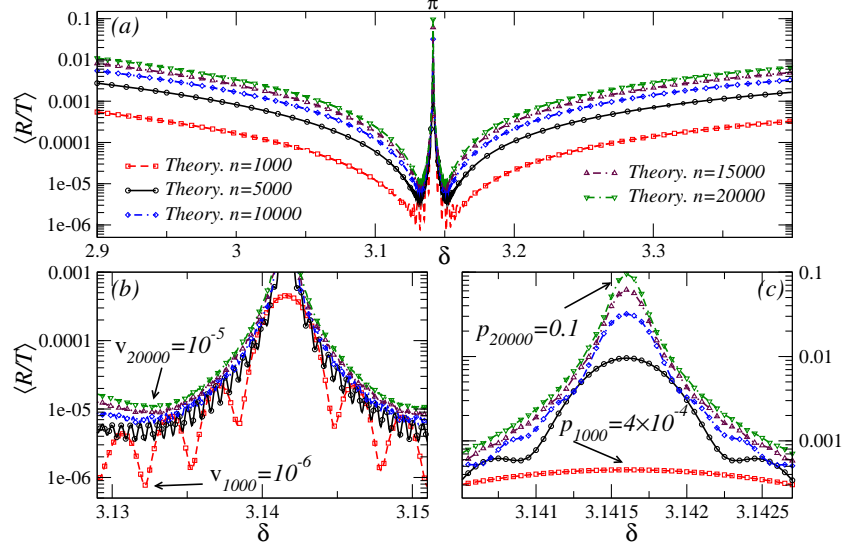


FIG. 8: Theoretical calculations of $\langle R/T \rangle$ vs δ for $y_0 = 0.09$, well inside regime II, for $n = 1000, 5000, 10000, 15000, 20000$, to show that the peak (p) to valley (v) ratio p/v increases with n : for $n=1000$, $p/v \sim 400$; for $n=20000$, $p/v \sim 10^4$. The peak is to be seen in panel (c) and the valley in panel (b). Going from (a) to (b) to (c), the δ interval was taken to be ever smaller. We also observe from the figure that τ_δ decreases with n , as predicted by Eq. (3.20).

In terms of the polar representation⁷ already employed in previous sections, i.e., $\lambda_r = |\beta_r|^2$ for the r -th scatterer and $\lambda^{(n)} = |\beta^{(n)}|^2$ for the chain consisting of n scatterers, Eq. (4.1) becomes

$$\frac{\partial \langle \lambda \rangle_s}{\partial s} = 1 + 2 \langle \lambda \rangle_s, \quad (4.2)$$

where

$$s = nl_c/\ell = L/\ell. \quad (4.3)$$

This “evolution” with s of $\langle \lambda \rangle_s$ coincides with that found from the evolution equation for the λ probability density, $w_s(\lambda)$, known as Melnikov’s equation^{7,22}

$$\frac{\partial w_s(\lambda)}{\partial s} = \frac{\partial}{\partial \lambda} \left[\lambda(1 + \lambda) \frac{\partial w_s(\lambda)}{\partial \lambda} \right]. \quad (4.4)$$

We *propose* the validity of Melnikov’s equation for regime I and verify the consequences numerically. In particular, from this assumption we can find the statistical properties of the transmission coefficient T which, in terms of λ , can be written as

$$T = \frac{1}{1 + \lambda}; \quad (4.5)$$

indeed, from Melnikov's equation (4.4), the expression for the p -th moment of T can be reduced to quadrature, with the result¹⁶

$$\langle T^p \rangle = \frac{2e^{-\bar{s}/4}}{\Gamma(p)} \int_0^\infty e^{-\bar{s}t^2} \left| \Gamma \left(p - \frac{1}{2} + it \right) \right|^2 t \tanh(\pi t) dt, \quad (4.6)$$

from which we find the first moment as

$$\langle T \rangle = 2e^{-\bar{s}/4} \int_0^\infty e^{-\bar{s}t^2} \pi t [\tanh(\pi t) / \cosh(\pi t)] dt. \quad (4.7)$$

In Fig. 9 we compare result (4.7) with numerical simulations obtained for various values of δ in regime I as a function of the length n of the chain: the agreement is excellent, indicating that the approximation involved in using Melnikov's equation is reasonable.

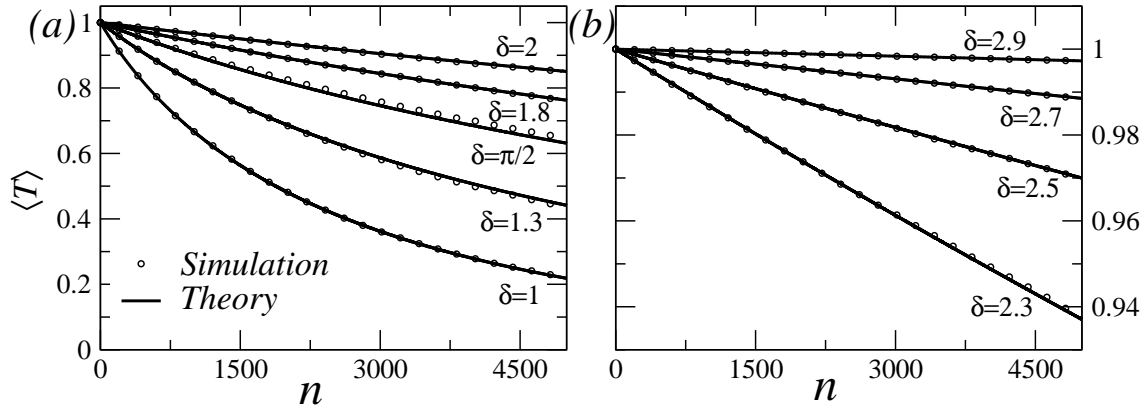


FIG. 9: Theory and numerical simulations for the average transmission coefficient $\langle T \rangle$ as a function of the number n of scatterers and for various values of the phase parameter δ in regime I, in the range: (a) $1 < \delta < 2$, and (b) $2.3 < \delta < 2.9$, as in Fig. 3. For the simulation, an ensemble of 10^4 realizations was used. As usual, we chose the parameter $y_0 = 0.09$. The theoretical results, obtained from Eq. (4.7), lie on top of the numerical ones. The error bar due to the finite sample is not indicated in the figure: e. g., for $\delta = \pi/2$ and $n = 5000$, the error is $\sim 10^{-2}$.

B. Average Landauer-Büttiker conductance in regime II as function of the number of scatterers n

In regime II, the theoretical analysis uses the approximation (see Eq. (2.7b))

$$\langle T \rangle \approx 1 - \langle \lambda \rangle, \quad (4.8)$$

since $\langle \lambda \rangle \ll 1$ (see Fig. 7), and $\langle \lambda \rangle$ is obtained from the results of the previous section, which make use of the exact recursion relation (3.6) and diagonalization of the matrix Ω . The results, together with numerical simulations, are shown in Fig. 10 for $\delta = \pi$, and in Fig. 11 for $\delta = \pi$ and very close to π . From the excellent agreement we see that our basic approximation, Eq. (4.8), appears justified.

Again, the oscillations shown in Fig. 11 are a novel feature of these results, arising from finite-size scatterers. The period τ_n of the oscillations can be taken over from the footnote to Fig. 6 and is consistent with what we observe in Fig. 11.

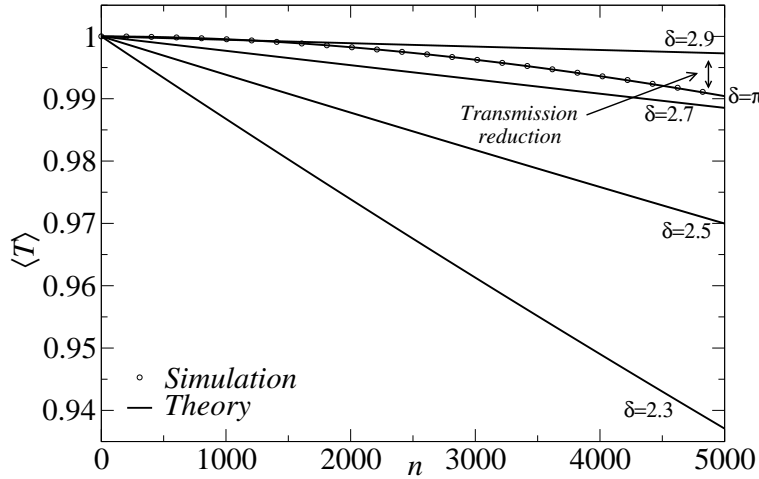


FIG. 10: For the same system as in Fig. 9(b), theoretical results from Eq. (4.8) and computer simulations are shown, for $\delta = \pi$. The agreement is excellent. Theoretical results in the interval $2.3 < \delta < 2.9$ (regime I), taken from Fig. 9(b), are also shown for comparison. The system is less delocalized for $\delta = \pi$ than for $\delta = 2.9$. As a result, the transmission is “reduced” as $\delta = \pi$ is approached..

C. Average Landauer-Büttiker conductance in regimes I and II, as function of δ for fixed n

Just as we did in the case of the resistance in Sec. III C, we now analyze the behavior of the average conductance $\langle T \rangle$ for a fixed length n of the chain, as a function of the phase parameter δ . Fig. 12 shows the analytical and numerical results for $n = 5000$ scatterers and $2.5 < \delta < 4$, covering regimes I and II. In regime I, the analytical results are obtained from Eq. (4.7), which gives an excellent description of the data. In regime II, the analytical results are obtained from Eq. (4.8) and $\langle \lambda \rangle$ is extracted from the results of Sec. III.

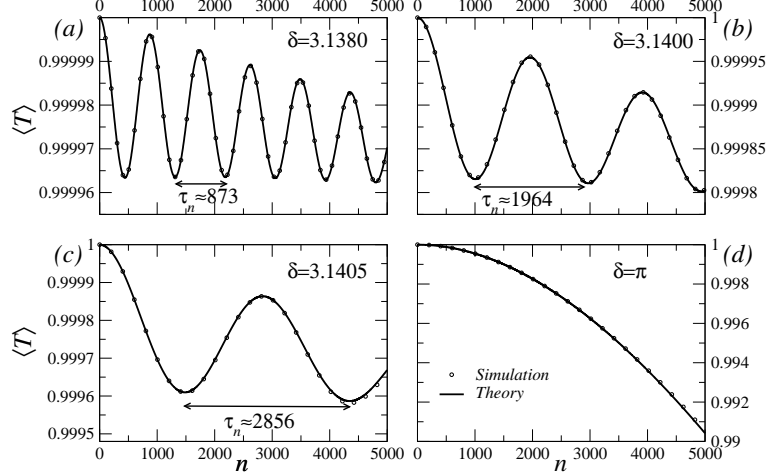


FIG. 11: The theoretical average transmission coefficient $\langle T \rangle$ vs. n , obtained from the approximation of Eq. (4.8), for $y_0 = 0.09$ and for four values of $\delta \approx \pi$: (a)-(c) $\delta = 3.1380, 3.1400, 3.1405$; (d) $\delta = \pi$ (as in Fig. 6), compared with numerical simulations. The agreement is excellent, suggesting that the approximation of Eq. (4.8) is justified. The estimate from Eq. (3.19) of the period τ_n of the oscillations is indicated in each panel and is consistent with the analytical results and the numerical simulations.

Fig. 12 shows that the average conductance exhibits a “gross-structure” in the form of a “bump”. For the case of weak scatterers, the system is almost transparent in regime II, and regime I is more localized. This gross-structure behavior is not entirely surprising. A single barrier with fixed width and strength becomes completely transparent ($T = 1$) at the resonance values $\bar{k}l_c = n\pi$, $n = 1, 2, \dots$, where \bar{k} is the wave number in the region of the barrier ($\delta \gtrsim \pi$ for low barriers). For a well, $T = 1$ at $\delta \lesssim \pi$. For a fixed step width and random strength with zero average, and still for $n = 1$, $\langle T \rangle$ reaches a maximum value smaller than unity at $\delta = \pi$. As the number of scatterers n increases, the gross structure seen in $\langle T \rangle$ as a function of δ is still similar to the above description for one random scatterer, in that *regime II* ($\delta \sim \pi$) shows *the system to be almost transparent* and less localized than in regime I. However, the trend of the system to delocalize as it approaches $\delta = \pi$ from both sides reverses in an extremely narrow window around $\delta = \pi$: indeed, for $\delta \approx \pi$, Fig. 12 shows the existence of an “*incipient forbidden region*”, which becomes ever more conspicuous as n increases. As a result, the average conductance suffers a dramatic reduction, with a peak to valley ratio that increases with n . This is consistent with the behavior of $\langle R/T \rangle$ that we already noticed in Figs. 7 and 8.

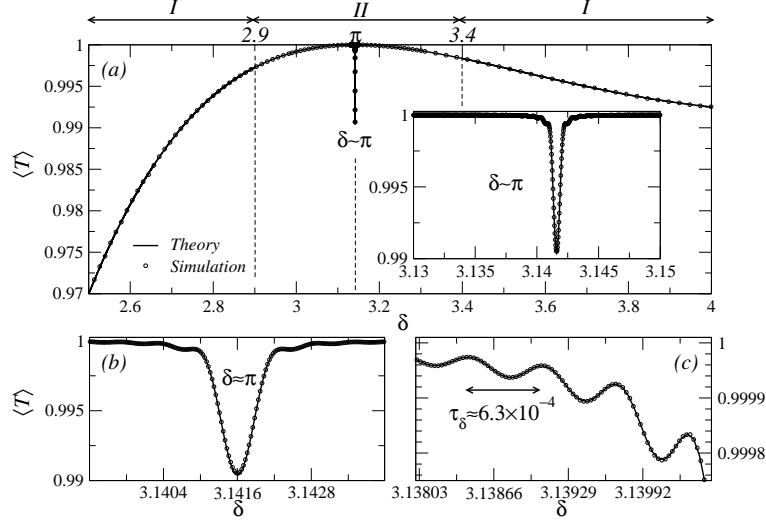


FIG. 12: Theoretical results (as described in the text) and numerical simulations for $\langle T \rangle$ vs δ in Regimes I and II, for a chain of $n = 5000$ scatterers and 10^5 realizations. The main figure shows the “gross-structure” behavior and the dip for $\delta \approx \pi$ exhibiting an “incipient forbidden region”: a zoom of the latter is shown in the insets. The agreement between simulation and theory is excellent. Notice the interference fringes in the inset; the period τ_δ of the oscillations was estimated using Eq. (3.20) and agrees well with the data (in spite of δ being quite close to π). The statistical error bar for $\delta = \pi$ is $\sim 10^{-5}$.

This incipient forbidden region has a number of features in common with those observed for a finite stretch of a periodic Kronig-Penney potential: i) it becomes deeper as n increases, ii) it becomes wider as the strength of the potential increases (this we verified by changing y_0), iii) it shows interference fringes at the edges, as seen in the inset of Fig. 12.

As for the value of δ around which the forbidden regions appears, $\delta = \pi$ occurs in the particular case where $\langle V_r \rangle = 0$. When all the potentials are barriers, i.e., $V_r > 0$, the “bump” and the forbidden region move to $\delta > \pi$; when all the potentials are wells, i.e., $V_r < 0$, the “bump” and the forbidden region move to $\delta < \pi$.

V. CONCLUSIONS

To summarize, we have discussed the problem of electronic transport in 1D disordered conductors, where the impurities consist of n weak barriers and wells having a finite, constant width l_c , and random strength. For the calculation of the average Landauer resistance, the problem is reduced to the diagonalization of a three-dimensional complex symmetric matrix.

Approximate results can be obtained analytically, by truncating the matrix when the phase parameter $\delta = kl_c$ is very far from π (regime I). In regime II, the method is improved by using perturbation theory when δ is not too close to π . When $\delta \approx \pi$ (well inside regime II), the diagonalization was done numerically, giving essentially exact results. The average conductance was calculated approximately, making use of Melnikov's equation in regime I and, in regime II, using the results obtained for the resistance. The theoretical results were verified in the two regimes using computer simulations.

In regime I, the average Landauer resistance was found, for a fixed δ , to increase exponentially with n . The mfp depends on δ : as δ increases towards π , both the average Landauer resistance and the average conductance show that the system becomes more delocalized.

As we enter regime II, a new feature appears, compared with older calculations: the transport properties show an oscillatory behavior as functions of n and/or δ , which we could explain using perturbation theory.

Well inside regime II ($\delta \approx \pi$), a second novel phenomenon shows up: we found an incipient "forbidden region", where i) the average conductance suffers a dramatic reduction, and ii) the average Landauer resistance increases by various orders of magnitude. In this region, a small change in δ modifies drastically the transport behavior as a function of n .

The novel phenomena we found and the success of our theoretical analysis in their description suggest the importance of the system's experimental realization.

Acknowledgments

M.Y. is grateful to the IFUNAM for its hospitality during the development of this work; he also acknowledges technical support in computer simulations from C. López Natarén. PAM acknowledges support from Conacyt, under Contract 79501, and from DGAPA, under Contract PAPIIT IN109014.

Appendix A: Diagonalization of the matrix Ω , Eqs. (3.4).

The matrix Ω is complex symmetric; provided it has no double characteristic values, it can be diagonalized by a *complex orthogonal transformation*: calling

$$D = \begin{bmatrix} \mu_1 & 0 & 0 \\ 0 & \mu_2 & 0 \\ 0 & 0 & \mu_3 \end{bmatrix} \quad (\text{A1})$$

the matrix of eigenvalues and O the complex orthogonal matrix whose columns are the eigenvectors of Ω , we have

$$\Omega = O D O^T. \quad (\text{A2})$$

The new vector

$$z'(n) = O^T z(n) \quad (\text{A3})$$

has the particularly simple solution

$$z'(n) = D^n z'(0), \quad (\text{A4a})$$

with components

$$z'_a(n) = (\mu_a)^n z'_a(0). \quad (\text{A4b})$$

The original vector $z(n)$ can thus be expressed as

$$z(n) = (O D^n O^T) z(0). \quad (\text{A5})$$

The first component of this equation gives Eq. (3.6a).

Appendix B: Perturbation theory

If we express $A(n)$ of Eq. (3.16) as

$$A(n) = \sum_{a=1}^3 A^{(a)}(n) \quad (\text{B1a})$$

$$A^{(a)}(n) = (\mathbf{v}_a)_1^2 \mu_a^n, \quad (\text{B1b})$$

we can write

$$\log A^{(a)}(n) = \log[(\mathbf{v}_a)_1^2] + n \log \mu_a. \quad (\text{B2})$$

The first term in Eq. (B2) and the coefficient of n are the two parameters of a straight line representing $\log A^{(a)}(n)$ as a function of n . If we develop perturbation theory in the eigenvalues and eigenvectors of Ω so as to give corrections of the same order in $\Delta\Omega$ in both terms of Eq. (B2), we shall be building a *consistent approximation to the two parameters that define the straight line* that we have just described. A perturbation theory with this criterion is briefly developed in what follows and used in the main text. The theory is taken over, almost *verbatim*, from the perturbation theory developed in any textbook on Quantum Mechanics, being careful to consider Ω not as a Hermitean matrix, but as a complex-symmetric matrix.

If we write for the eigenvalues μ_i of Eq. (3.15) the expansion

$$\mu_i = \mu_i^{(0)} + \mu_i^{(1)} + \mu_i^{(2)} + \cdots, \quad (\text{B3})$$

we find

$$\mu_i^{(0)} = \begin{cases} 1, & i = 1 \\ e^{2i\delta}, & i = 2 \\ e^{-2i\delta}, & i = 3 \end{cases} \quad (\text{B4a})$$

$$\mu_i^{(1)} = \Delta\Omega_{ii} \quad (\text{B4b})$$

$$\mu_i^{(2)} = \sum_{j(\neq i)} \frac{\Delta\Omega_{ij}\Delta\Omega_{ji}}{\mu_i^{(0)} - \mu_j^{(0)}} \quad (\text{B4c})$$

...

Similarly, for the eigenvectors \mathbf{v}_i of Ω we write the expansion

$$\mathbf{v}_i = \mathbf{v}_i^{(0)} + \mathbf{v}_i^{(1)} + \mathbf{v}_i^{(2)} + \cdots, \quad (\text{B5})$$

and find

$$\mathbf{v}_i^{(0)} = \begin{cases} (1, 0, 0)^T, & i = 1 \\ (0, 1, 0)^T, & i = 2 \\ (0, 0, 1)^T, & i = 3 \end{cases} \quad (\text{B6a})$$

$$\mathbf{v}_i^{(1)} = \sum_{j(\neq i)} \frac{\Delta\Omega_{ji}}{\mu_i^{(0)} - \mu_j^{(0)}} \mathbf{v}_j^{(0)} \quad (\text{B6b})$$

$$\begin{aligned} \mathbf{v}_i^{(2)} = & \sum_{j,k(\neq i)} \frac{\Delta\Omega_{jk}\Delta\Omega_{ki}}{(\mu_i^{(0)} - \mu_j^{(0)})(\mu_i^{(0)} - \mu_k^{(0)})} \mathbf{v}_j^{(0)} \\ & - \sum_{j(\neq i)} \frac{\Delta\Omega_{ii}\Delta\Omega_{ji}}{(\mu_i^{(0)} - \mu_j^{(0)})^2} \mathbf{v}_j^{(0)} - \frac{1}{2} \left[\sum_{j(\neq i)} \frac{\Delta\Omega_{ij}\Delta\Omega_{ji}}{(\mu_i^{(0)} - \mu_j^{(0)})^2} \right] \mathbf{v}_i^{(0)} \\ & \dots \end{aligned} \quad (\text{B6c})$$

Appendix C: Reduction to the results of the dense weak-scattering limit

In this appendix we briefly investigate the limit in which the results of the present model—consisting of finite-size scatterers—reduce to those obtained in the dense weak-scattering limit (DWSL) of Ref.⁸, consisting of a succession of delta scatterers.

1. The present model

A barrier lower than the energy requires (see Eq. (2.3)) $y_r < \delta^2$, so that very weak barriers are characterized by $y_0 \ll \delta^2$. We further require the wavelength λ to be much larger than the barrier width l_c , i.e., $\delta = kl_c \ll 1$. We thus have the joint requirements

$$y_0 \ll \delta^2 \ll 1. \quad (\text{C1})$$

Eq. (3.13) for the mfp (designated here by ℓ) can be written in the equivalent ways

$$\frac{1}{k\ell} = \frac{y_0^2}{12\delta^3}, \quad (\text{C2a})$$

$$\eta \equiv \frac{1}{\nu\ell} = \frac{y_0^2}{12\delta^2}, \quad (\text{C2b})$$

$$\delta = \frac{y_0}{\sqrt{12\eta}}, \quad (\text{C2c})$$

$$\frac{1}{k\ell} = \frac{\eta}{\delta}, \quad (\text{C2d})$$

$\nu = 1/l_c$ being the density of scatterers. A problem is thus specified by the three parameters η , y_0 , δ , related by one of the above equations, like (C2c). To satisfy the inequality (C1) we need

$$12\eta \ll y_0 \ll \sqrt{12\eta} . \quad (\text{C3})$$

We follow the steps:

- i) propose $\eta \ll 1$;
- ii) propose y_0 to be consistent with (C3); this is used to set up the numerical barrier model.
- iii) find δ from (C2c).

2. The DWSL model

The DWSL model of Ref.⁸ consists of a succession of equally spaced (spacing = d) delta potentials, with an rms intensity u_0 , having units of k .

The relation defining the mfp can also be written in various equivalent ways

$$\frac{1}{k\ell} = \frac{u_0^2}{12k^3d} , \quad (\text{C4a})$$

$$= \frac{v_0^2}{3kd} , \quad (\text{C4b})$$

$$\frac{d}{\ell} = \frac{v_0^2}{3} . \quad (\text{C4c})$$

Here, d is the distance between successive delta potentials and $v_0 = u_0/2k$.

In this model, too, the problem is specified by three parameters: $k\ell$, kd , v_0 , related by one of the above equations, like (C4c).

3. Connection between the two models

We need to connect the two models:

- i) choose $k\ell$ to be the same in the two models
- ii) choose kd of the DWSL delta-potential model to coincide with $kl_c = \delta$ of the finite-size scatterer model. This implies that the fraction of wavelength contained in the interval between the centroids of two successive scatterers is the same in the two models (compare Fig. 1 of the present paper with Fig. 3 of Ref.⁸).

iii) from kd and $k\ell$ we find d/ℓ and hence v_0 from Eq. (C4c), which is to be used to set up the numerical delta-potential model.

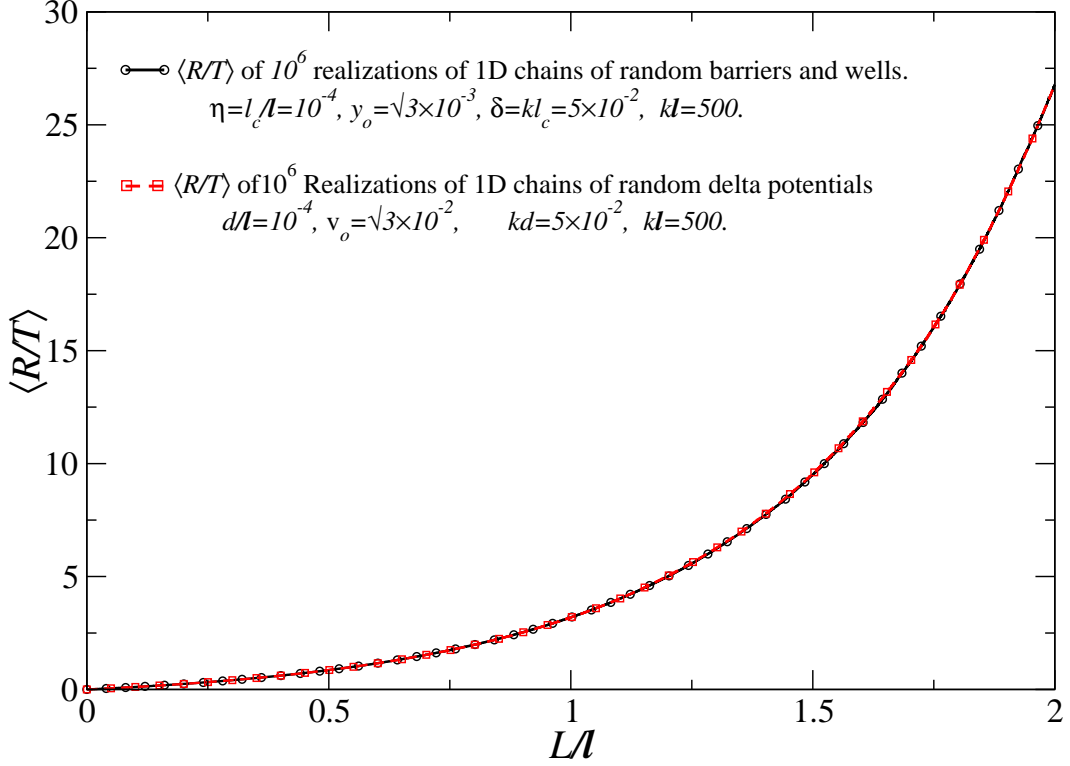


FIG. 13: Results of computer simulations for the average Landauer resistance for the present model and the DWSL model of Ref.⁸. The parameters chosen for each model are indicated in the figure, and conform to the criteria explained in the text. The agreement is excellent.

Fig. 13 shows computer simulations for the average Landauer resistance for the two models as a function of L/ℓ , L being the length of the chain, for the parameters indicated in the figure. The agreement is excellent. This figure is similar to Fig. 3 of Ref. [8].

-
- ¹ P. W. Anderson, *Phys. Rev.* **109**, 1492 (1958).
 - ² I. M. Lifshitz, S. A. Gredeskul and L. A. Pastur, *Introduction to the Theory of Disordered Systems*, J. Wiley, N.Y., 1988.
 - ³ P. Sheng, (ed.)(1990). *Scattering and localization of classical waves in random media*. World Scientific, Singapore.
 - ⁴ B. L. Altshuler, P. A. Lee and R. A. Webb, (ed.)(1991). *Mesoscopic phenomena in solids*. North-Holland, Amsterdam.
 - ⁵ C. W. J. Beenakker and H. van Houten, (1991). *In Solid state physics* (ed. H. Ehrenreich and D. Turnbull), p. 1. Volume 44. Academic press, New York.
 - ⁶ N. F. Mott and W. D. Twose, *Adv. Phys.*, **10**, 107 (1961)
 - ⁷ P. A. Mello and N. Kumar, *Quantum Transport in Mesoscopic Systems. Complexity and Statistical Fluctuations* (Oxford University Press, 2010)
 - ⁸ L. S. Froufe-Pérez, M. Yépez, P. A. Mello, and J. J. Sáenz, *Phys. Rev. E*, **75**, 031113 (2007).
 - ⁹ D. H. Dunlap, H-L. Wu, and P. W. Phillips, *Phys. Rev. Lett.* **65**, 88 (1990); P. Phillips and H-L. Wu, *Science* **252**, 1805 (1991).
 - ¹⁰ A. Bovier, *J. Phys. A* **25**, 1021 (1992).
 - ¹¹ J. C. Flores and M. Hilke, *J. Phys. A* **26**, L1255 (1993); M. Hilke, *J. Phys. A* **27**, 4773 (1994); M. Hilke and J. C. Flores, *Phys. Rev. B* **55**, 10625 (1997).
 - ¹² S. N. Evangelou and E. N. Economou, *J. Phys. A* **26**, 2803 (1993).
 - ¹³ F. M. Izrailev and A. A. Krokhin, *Phys. Rev. Lett.* **82**, 4062 (1999); A. Sánchez, F. Domínguez-Adame, G. Berman and F. Izrailev, *Phys. Rev. B* **51**, 6769 (1995); U. Kuhl, F.M. Izrailev, and A. A. Krokhin, *Phys. Rev. Lett.* **100**, 126402 (2008); J.C. Hernández-Herrejón, F.M. Izrailev, and L. Tessieri, arXiv:1003.3691 [cond-mat.dis-nn].
 - ¹⁴ F. A. B. F. de Moura and M. L. Lyra, *Phys. Rev. Lett.* **81**, 3735 (1998).
 - ¹⁵ M. Titov and H. Schomerus, *Phys. Rev. Lett.* **95**, 126602 (2005).
 - ¹⁶ M. Díaz, P. A. Mello, M. Yépez and S. Tomsovic, *Europh. Lett.* **97**, 54002 (2012).
 - ¹⁷ I. F. Herrera-González, F. M. Izrailev and N. M. Makarov, *Phys. Rev. E* **88**, 052108 (2013).
 - ¹⁸ C. S. Kim, A. M. Satanin, Y. S. Joe, and R. M. Cosby, *Phys. Rev. B* **60**, 10962 (1999); J.H. Bardarson, I. Magnúsdóttir, G. Gudmundsdóttir, C-S Tang, A. Manolescu, and V. Gudmunds-

- son, Phys. Rev. B **70**, 245308 (2004); V. Vargiamidis and H. M. Polatoglou, Phys. Rev. B **72**, 195333 (2005), and Phys. Rev. B **75**, 153308 (2007); H. Zheng, Z. Wang, Q. Shi, and X. Wang, Phys. Rev. B **74**, 155323 (2006).
- ¹⁹ R. Landauer, *Philos. Mag.* **21**, 863 (1970).
- ²⁰ M. Büttiker, *IBM Res. Dev.* **32**, 317 (1988).
- ²¹ G. García Calderón, Phys. Rev. B **56**, 4845 (1997), Phys. Rev. A **79**, 052103 (2009), and *private communication*.
- ²² V.I. Mel'nikov, *Pis'ma Zh. Eksp. Teor. Fiz.*, **32**, 244 (1980). [*JETP Lett.*, **32**, 225. (1980)]; *Fiz. Tverd. Tela (Leningrad)*, **23**, 782 (1981). [*Sov. Phys. Solid State*, **23**, 444. (1981)].